Calhoun: The NPS Institutional Archive

DSpace Repository

NPS Scholarship | Publications

1991-10

Wake Measurements and Loss Evaluation in a Controlled Diffusion Compressor Cascade

Shreeve, R. P.; Elazar, Y.; Dreon, J. W.; Baydar, A.

https://hdl.handle.net/10945/36778

This publication is a work of the U.S. Government as defined in Title 17, United States Code, Section 101. Copyright protection is not available for this work in the United States.

Downloaded from NPS Archive: Calhoun

http://www.nps.edu/library

Calhoun is the Naval Postgraduate School's public access digital repository for research materials and institutional publications created by the NPS community. Calhoun is named for Professor of Mathematics Guy K. Calhoun, NPS's first appointed -- and published -- scholarly author.

Dudley Knox Library / Naval Postgraduate School
411 Dyer Road / 1 University Circle
Monterey, California USA 93943

R. P. Shreeve

Y. Elazar

J. W. Dreon

A. Baydar

Turbopropulsion Laboratory,
Naval Postgraduate School,
Monterey, CA 93943

Wake Measurements and Loss Evaluation in a Controlled Diffusion Compressor Cascade

The results of two component laser-Doppler velocimeter (LDV) surveys made in the near wake (to one fifth chord) of a controlled diffusion (CD) compressor blade in a large-scale cascade wind tunnel are reported. The measurements were made at three positive incidence angles from near design to angles thought to approach stall. Comparisons were made with calibrated pressure probe and hot-wire wake measurements and good agreement was found. The flow was found to be fully attached at the trailing edge at all incidence angles and the wake profiles were found to be highly skewed. Despite the precision obtained in the wake velocity profiles, the blade loss could not be evaluated accurately without measurements of the pressure field. The blade trailing edge surface pressures and velocity profiles were found to be consistent with downstream pressure probe measurements of loss, allowing conclusions to be drawn concerning the design of the trailing edge.

Introduction

Controlled diffusion (CD) blading shapes were introduced into the design systems for axial compressors only a few years ago (Hobbs and Weingold, 1984). The CD blade contour, for a given inlet air angle, turning angle, solidity, and streamline contraction, is usually the result of an inviscid design process operated sequentially or interactively with surface boundary layer predictions. The resulting blade shape is one on which the suction-side boundary layer is predicted not to separate at design conditions (Sanger, 1983). The inviscid-plus-boundary layer design procedure results in shapes that can have significant (but controllable) trailing edge thicknesses where a Kutta condition has been imposed (Hobbs and Weingold, 1984; Sanz, 1988). The closing of the trailing edge shape, with a radius for example, is a matter of some judgment since a generalized model of a compressor blade base flow suitable for design purposes has not been established. The need for such modeling has previously stimulated both cascade (Hobbs et al., 1982) and large-scale trailing edge simulation studies (Patersen and Weingold, 1985; McCormick et al., 1988). However, the understanding that can be obtained from single experiments on specific designs is necessarily limited and an assimilation of the information from a range of experiments could lead to much greater insight. It is in this spirit that the present results are reported.

The present work began with an experimental program aimed at verifying an inviscid-plus-boundary layer method for designing CD compressor blading (Sanger, 1983). The comparison of experimental with design and predicted off-design performance of a particular CD cascade (hereafter referred to as the Sanger cascade) was reported (Sanger and Shreeve, 1986), and it was clear from the study that off-design and stalling behavior were not predicted adequately using boundary-layer codes. In order to provide detailed experimental data with which to assess existing and developing viscous codes, in particular their ability to predict stall, a complete mapping of the flow through the cascade was made using a two-component laser-Doppler velocimeter (LDV) at design and two higher incidence angles (Elazar, 1988). Preliminary assessments made by Elazar of boundary layer (McNally, 1970), interactive boundary layer (Snir, 1988), and Navier-Stokes (Shamroth et al., 1984) code predictions showed that only the Navier-Stokes code gave reasonable results. It was also clear however, that transition modeling was critical in obtaining the good agreement. The experimental results for the boundary layer devel-

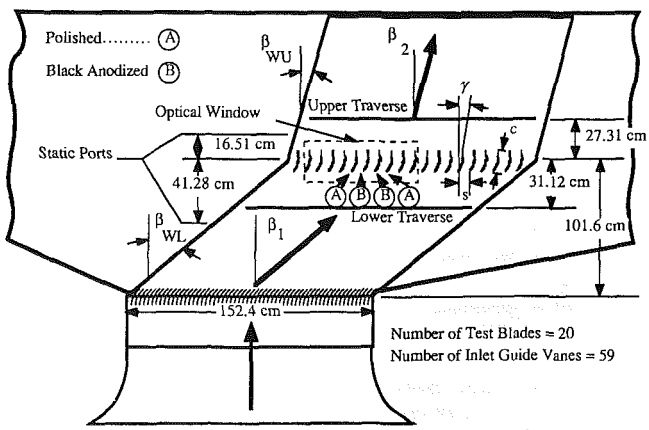

Fig. 1 Schematic of the cascade wind tunnel

Contributed by the International Gas Turbine Institute and presented at the 35th International Gas Turbine and Aeroengine Congress and Exposition, Brussels, Belgium, June 11–14, 1990. Manuscript received by the International Gas Turbine Institute February 7, 1990. Paper No. 90-GT-129.

Copyright © 1991 by ASME

Downloaded From: http://turbomachinery.asmedigitalcollection.asme.org/ on 09/03/2013 Terms of Use: http://asme.org/terms

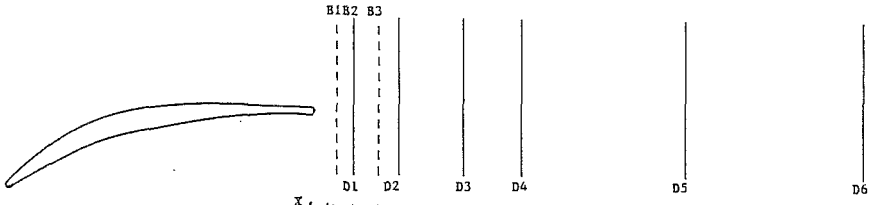

SURVEY STATIONS

Y/c	LDV	HOT-WIRE	PRESSURE PROBE
0.052	E1	-	-
0.072	E2	-	-
0.080	-	B1	-
0.135	E3	B2	D1
0.212	E4	B3	-
0.277	-	-	D2
0.485	-	-	D3
0.669	-	-	D4
1.197	-	-	D5
1.783	-	-	D6

Fig. 2 Cascade geometry and measurement locations

opment in the Sanger cascade with sufficient information to permit its use for preliminary code assessment purposes were given in an earlier paper (Elazar and Shreeve, 1990). A report containing all test results is to be issued (Shreeve and Elazar, 1989).

For code assessment, the Sanger cascade was found to provide a unique test case. The surprising feature of the flow field was that the suction side boundary layer was found to remain completely attached at the trailing edge at incidence angles that were thought from the loss measurements to be "stalling." A leading edge separation bubble was observed to grow as the incidence was increased, but losses could reach four times the minimum loss for the cascade (Classick, 1989) without the appearance of any trailing edge separation (Murray, 1989). This contrasts significantly with the behavior of a double-circular arc (DCA) compressor cascade, on which a similarly detailed mapping was made (Deutsch and Zierke, 1987, 1988; Zierke and Deutsch, 1990), wherein an unsteady separation occurred on the suction side at positive incidence angles.

In view of the steady and attached flow found at the trailing edge of the Sanger cascade, LDV measurements made in the blade wake are again useful as a well-prescribed test case for viscous calculations. The point must be made, however, that the LDV technique gives accurate measurements only of the velocity field. As was stated earlier (Elazar and Shreeve, 1990), the loss coefficient for the cascade could not be evaluated accurately from LDV data alone, and the uncertainty introduced by an assumption as to the pressure field was comparable in magnitude to the loss itself. In order to assess completely the ability of emerging viscous codes to predict off-design behavior, and in particular the losses (Davis et al., 1988), it is desirable to have equally accurate measurements of the velocity field and the losses.

Consequently, the present paper presents results of LDV measurements made in the wakes of the Sanger cascade at increasing incidence (Elazar, 1988), and relates them to calibrated pressure probe (Dreon, 1986) and hot-wire probe (Baydar, 1988) measurements. The values obtained for the loss coefficient and the recovery of the static pressure from the lower values measured on the blade trailing edge are analyzed and are shown to be consistent with the effect of wake mixing.

Test Facility and Instrumentation

The subsonic cascade wind tunnel and operating instrumentation were as described by Sanger and Shreeve (1986). The configuration of the wind tunnel is shown in Fig. 1. The tests involved 20 test blades across a test section width of 1.524 meters. The blade span was 25.4 cm. Inlet air angle was adjusted by rotating the lower side walls and inlet guide vanes. The test blading was mounted to a rack, which translated to a new position as the angle was changed. At each angle the outlet end walls were adjusted so that the downstream wall static pressure was atmospheric and nearly uniform in the blade-to-blade direction. The guide vane position was selected such that the wall static pressure was nearly uniform in the blade-to-blade direction. An upstream blade-to-blade survey using a calibrated five-hole pressure probe verified near uniformity of the flow over six blade passage widths. Examples of profiles showing the degree of uniformity and periodicity of the flow field are given by Sanger and Shreeve (1986) and Elazar and Shreeve (1990). It is important to note that the 59

Nomenclature

AVDR = axial velocity-density ratio
c = blade chord = 12.73 cm
C_p = pressure coefficient
d = distance normal to the blade surface
d_{te} = diameter of the trailing edge
D = NASA diffusion factor
k = defined in equation (6)
M = Mach number
P = pressure
q = dynamic pressure
Re = Reynolds number
s = blade spacing
u = velocity component parallel to blade surface
v = velocity component normal to blade surface
V = velocity
X = transverse (horizontal) displacement
Y = axial (vertical) displacement
β = air angle defined in Fig. 1
δ^* = displacement thickness
Δ = defined in equation (5)
ξ = blade coordinate defined in Table 1
η = blade coordinate defined in Table 1
σ = solidity = c/s
$\bar{\omega}$ = mass-averaged loss coefficient

Subscripts

c = chord
min = minimum
p = pressure side
ref = reference, upstream
s = suction side
t = stagnation
te = trailing edge station
wu = upper wall of cascade
wl = lower wall of cascade
1 = upstream
2 = downstream

Downloaded From: http://turbomachinery.asmedigitalcollection.asme.org/ on 09/03/2013 Terms of Use: http://asme.org/terms

Table 1 Blade coordinates, cascade geometry and nominal test conditions

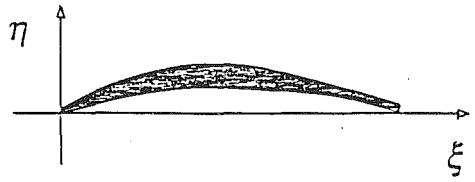

ξ (mm)	η (pressure side) (mm)	η (suction side) (mm)
0.000	0.114	0.114
0.056	———	0.213
0.145	0.005	———
0.564	0.112	0.498
1.128	0.257	0.780
1.692	0.394	1.024
2.256	0.526	1.240
2.819	0.648	1.425
3.383	0.759	1.577
3.947	0.838	1.684
4.511	0.889	1.755
5.075	0.912	1.791
5.639	0.912	1.798
6.203	0.894	1.781
6.767	0.869	1.730
7.330	0.841	1.651
7.894	0.805	1.549
8.458	0.765	1.430
9.022	0.714	1.295
9.586	0.653	1.151
10.150	0.577	0.998
10.714	0.485	0.843
11.278	0.371	0.686
11.841	0.226	0.528
12.405	0.048	0.368
12.510	0.010	———
12.609	———	0.310
12.725	0.157	0.157

Blade Type	Controlled Diffusion
Number of Blades	20
Blade Spacing	7.62 cm
Chord	12.73 cm
Solidity	1.67
Leading Edge Radius	0.114 cm
Trailing Edge Radius	0.157 cm
Thickness	7%
Setting Angle	14.2 ° ± 0.1 °
Stagger Angle	14.4 ° ± 0.1 °
Span	25.40 cm
NOMINAL TEST CONDITIONS	
Reynolds No.(chord)	720,000
Inlet	
Total Temperature	294 K
Total Pressure	1.03 ATM
Mach Number	0.25
Exit	
Static Pressure	1.00 ATM

inlet guide vanes, spaced only 2.54 cm apart, generated wakes that were well mixed and barely detectable just ahead of the test blades. The free-stream turbulence level was measured consistently to be 1.4 ± 0.7 percent.

The geometry of the cascade and axial locations of blade-to-blade surveys (made at midspan) are shown in Fig. 2. The geometry of the cascade is given in Table 1.

Data presented herein are from three studies. LDV measurements were made by Elazar (1988) of the flow through the passage formed by blades 7 and 8 from the left-hand end in Fig. 1. The wake flow was measured behind blade 7 at stations E1–E4 in Fig. 2.

The LDV velocity field measurements were referred to an upstream (uniform) inlet velocity derived from LDV surveys 0.3 chord lengths "axially" upstream and plenum conditions at the time of the individual measurement (Elazar and Shreeve, 1989). Details of the TSI two-component LDV system are given in the cited reference.

Calibrated five-hole pressure probe measurements were made by Dreon (1986) in the wake of blade 10. Two United Sensor Corporation cylindrical probes (Model DA-125) were used at the stations labeled "upper traverse" and "lower traverse in Fig. 1. The "upper traverse" corresponds to Station D6 in Fig. 2. A United Sensor Corporation conical probe (Model DC-125) was used for wake surveys nearer to the blade, at stations D1–D5 shown in Fig. 2. The probes were calibrated (in a free jet) and used in a yaw-balanced mode (Dreon, 1986), establishing calibration surfaces for dimensionless velocity and pitch angle in terms of two pressure difference coefficients. A special yaw angle probe was also used to provide a reference for yaw angle measurements in the blade wakes.

Single component hot-wire measurements were made by Baydar (1988) at stations B1–B3 in Fig. 2 in the near wake of blade 10. The hot wire was calibrated in situ using a Prandtl probe at the same blade-to-blade location, well outside the

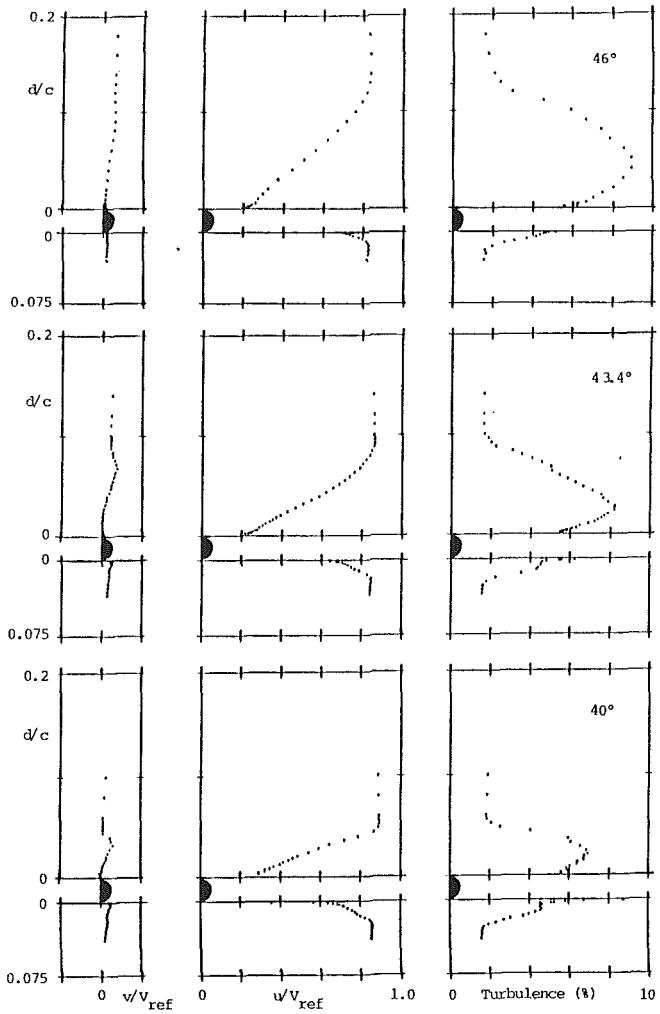

Fig. 3 Boundary layers measured at the blade trailing edge

wake, and with the two probe tips 2.54 cm on either side of the spanwise tunnel centerline. TSI anemometer (Model IFA-100), digitizer (Model IFA-200), and software (DAP) were used with an IBM PC-AT computer. Details of the measurements are given by Baydar (1988).

Results and Discussion

LDV Measurements. The results of two-component LDV surveys made in the blade-to-blade direction at the axial station of the center of radius at the blade trailing edge are shown in Fig. 3. The figure shows the axial (u) and transverse (v) components of the mean velocity and the turbulence level on the pressure and suction sides of the blade trailing edge, at three inlet air angles (40, 43.4, and 46 deg). The velocity components are shown as a ratio of the (uniform) inlet velocity. The turbulence level is also referred to the inlet (rather than to the local "free-stream") velocity. The displacement scale (from top to bottom) covers half a blade space, so that the extent of the viscous layer in relation to the blade passage can be easily appreciated. At an air inlet angle of 46 deg the two viscous layers and metal thickness are seen to occupy 35 percent of the area at the trailing edge.

It is interesting to note that there were significant differences in the behaviors of the boundary layers on the suction and pressure sides of the blade as incidence was increased (Elazar, 1988). On the suction side, the boundary layer increased in thickness as incidence was increased, but the turbulence profile showed that the layer retained the characteristics of a fully

Downloaded From: http://turbomachinery.asmedigitalcollection.asme.org/ on 09/03/2013 Terms of Use: http://asme.org/terms

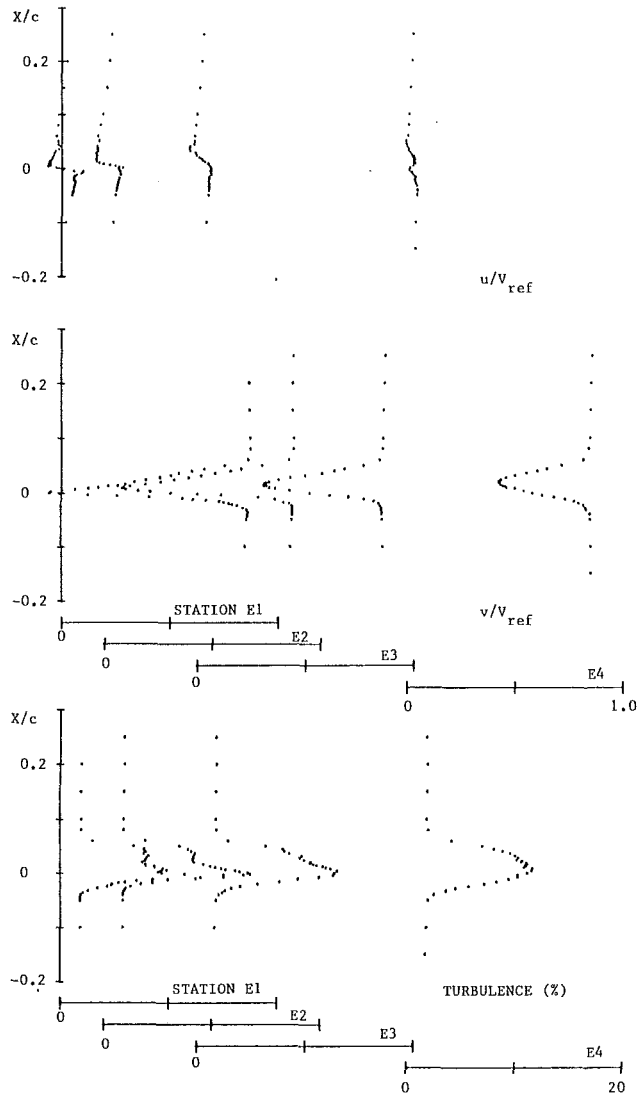

Fig. 4(*a*) LDV wake surveys at $\beta_1 = 40$ deg

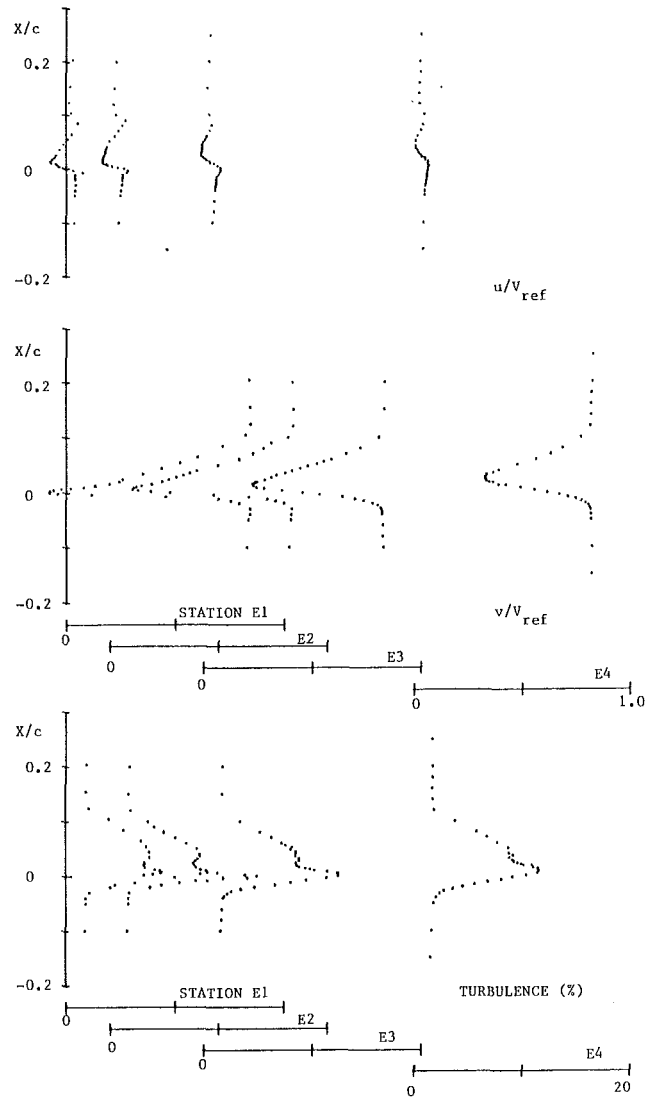

Fig. 4(*b*) LDV wake surveys at $\beta_1 = 43.4$ deg

turbulent boundary layer. On the pressure side, at inlet air angles of 40 and 43.4 deg, the velocity profiles were very similar to each other in every respect. At 46 deg however, the boundary layer was discernibly thinner and the turbulence levels within the layer decreased. These differences have to do with how transition occurred on the two sides of the blade. On the suction side, transition occurred over a laminar separation bubble near the blade leading edge. While the bubble grew as incidence was increased, reattaching at 46 percent chord at an air inlet angle of 46 deg, the boundary layer downstream of reattachment appeared always to be fully turbulent. On the pressure side of the blade, transition occurred naturally within the boundary layer over a significant fraction of the chord. Toward the trailing edge, the outer flow was accelerated significantly. The differences in stagnation point location, transition location and length, and acceleration toward the trailing edge as the incidence angle was changed, resulted in a significantly reduced boundary layer thickness on the pressure side of the blade at the highest inlet air angle of 46 deg.

The results of LDV surveys of the wake of the seventh blade are shown in Fig. 4. The surveys were made at distances $0.052c$, $0.072c$, $0.135c$, and $0.212c$, or, equivalently $2.15d_{te}$, $2.96d_{te}$, $5.56d_{te}$, and $8.7d_{te}$ (where d_{te} is the diameter at the blade trailing edge), downstream of the center of curvature of the trailing edge. The mean velocity components and the turbulence levels are shown in the figure.

It is first noted that the wake was, in general, highly asymmetric. The asymmetry was most pronounced at the station closest to the trailing edge, becoming less pronounced downstream, as mixing occurred. Only at $\beta_1 = 40$ deg, at the most downstream station ($8.7\ d_{te}$). was the wake nearly symmetric. Reversed flow was measured at $2.15d_{te}$ at $\beta_1 = 40$ deg and $\beta_1 = 43.4$ deg, but not at $\beta_1 = 46$ deg. Mixing was most rapid at $\beta_1 = 40$ deg. Figure 5 shows the variation in wake minimum velocity with distance downstream. It is interesting to note the differences that occurred at the three inlet flow angles. Since the pressure side boundary layers at the trailing edge were similar at $\beta_1 = 40$ deg and $\beta_1 = 43.4$ deg, it was possibly the thinner pressure side boundary layer at $\beta_1 = 46$ deg that led to a shorter reverse flow region at the highest angle.

The transverse velocity components approached $\pm$ 10 percent of the inlet velocity at the most upstream location ($2.15d_{te}$) and became almost constant at the most downstream station ($8.7d_{te}$). The constant value of approximately 1 percent of the inlet velocity was consistent with the presence of a small deviation angle.

The distributions of turbulence level show the wake asymmetry most clearly. The turbulence level was considerably higher (reaching 15 percent at $\beta_1 = 40$ deg), in the area of the wake containing the pressure side boundary layer. The suction

Downloaded From: http://turbomachinery.asmedigitalcollection.asme.org/ on 09/03/2013 Terms of Use: http://asme.org/terms

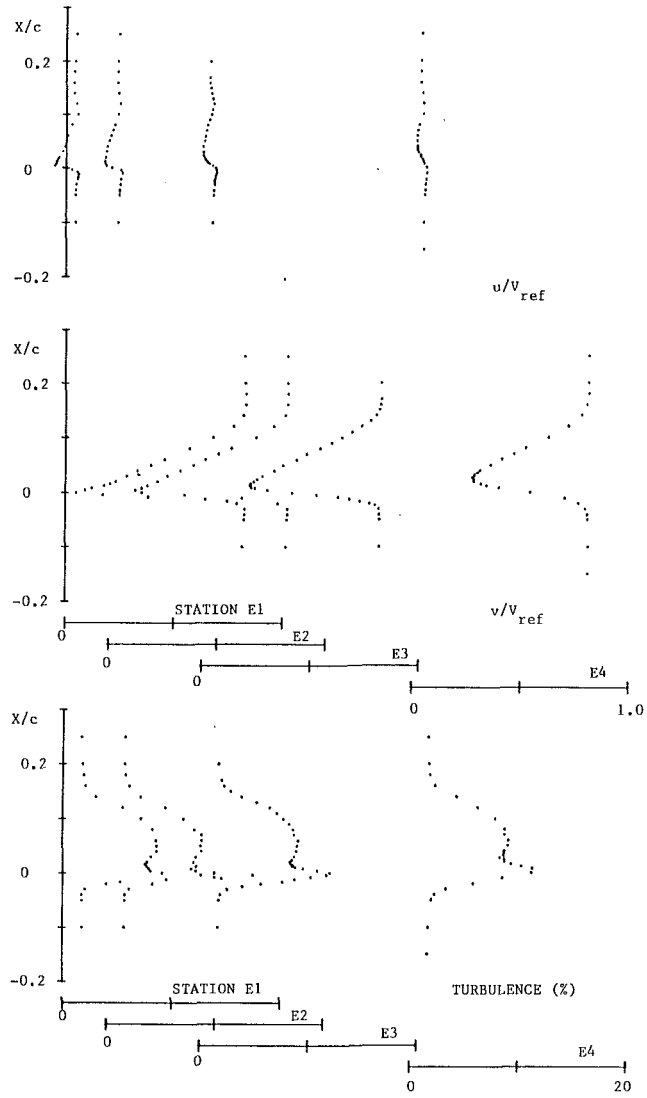

Fig. 4(c) LDV wake surveys at $\beta_1 = 46$ deg

side boundary layer generated turbulence in the wake of 8 percent or less.

Hot-Wire Measurements. Single component hot-wire measurements obtained by Baydar (1988) in the wake of the tenth blade are compared at corresponding axial stations with LDV measurements, made by Elazar (1988) in the wake of the seventh blade, in Fig. 6. In general, good agreement was obtained. Exceptional agreement was found in the mean velocity at $\beta_1 = 40$ deg. At $\beta_1 = 46$ deg, similar values of the minimum velocity were measured, but the hot wire showed the wake to be shifted slightly toward less deviation. Peak turbulence levels were in very good agreement at both $\beta_1 = 40$ deg and $\beta_1 = 46$ deg. However, the hot wire indicated somewhat higher turbulence levels than did the LDV in the region of the wake containing the suction-side boundary layer. No satisfactory explanation has been found for this difference. Since the hot wire could not be positioned with the equivalent accuracy that could be achieved with the LDV measurement volume, and since only the velocity magnitude could be obtained from the single wire, no further hot-wire measurements were made.

Pressure Probe Measurements. Measurements were made with a calibrated five-hole conical pressure probe behind the tenth blade at one axial station at which LDV measurements were made behind the seventh blade; namely, 0.135c downstream of the trailing edge center of radius. The measured velocity profiles are compared in Fig. 7 at $\beta_1 = 40$ deg and $\beta_1 = 43.4$ deg. Truly excellent agreement was seen at $\beta_1 = 40$ deg. At $\beta_1 = 46$ deg, some disagreement was evident, with the LDV measurements showing a somewhat wider and deeper wake. Two reasons for disagreement can be considered. First, the conical pressure probe was 0.32 cm in diameter and hence could interfere with the flow being measured in the very near wake. Unfortunately optical windows could not be installed at the tenth blade where the probe measurements were made so this could not be examined. It was noted that at $\beta_1 = 40$ deg, the wake was better mixed at the probe station, and interference might be less. Second, small differences might be present between the wakes of different blades at increased incidence angles. Since the wakes of the blades are developed from suction-side boundary layers, which develop downstream of growing separation bubbles, some differences are to be expected. Future experiments will examine this point more carefully. In general, the large number of test blades (20) circumvents the problem of achieving flow periodicity in the test section.

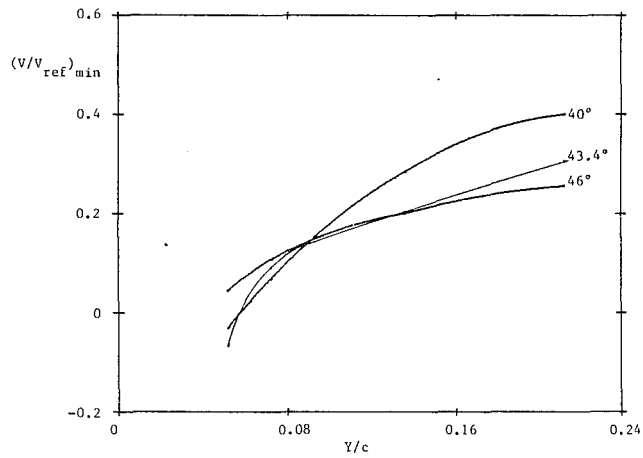

Fig. 5 Wake minimum velocity from LDV measurements

Wake velocity profiles measured by Dreon (1986) using the calibrated conical probe at five downstream stations and a calibrated cylindrical probe at the farthest downstream station are shown in Fig. 8 for $\beta_1 = 40$ deg and $\beta_1 = 43.4$ deg. The path of the wake minimum velocity away from the suction surface is shown in Fig. 9, where LDV data near to the trailing edge are included.

The total pressure profiles (the results of direct measurement of stagnation pressure at the tip of each probe) were qualitatively similar to the velocity profiles. From the velocity, stagnation pressure, and stagnation temperature (measured in the wind tunnel plenum) all properties of the flow were calculated at each location in the survey. By integration over one blade passage, values were obtained for the mass-averaged loss coefficient ($\bar{\omega}$, Sanger and Shreeve, 1986), the NASA diffusion factor (D), and the axial velocity-density ratio (AVDR) at each survey station. The results are shown in Fig. 10. Very consistent results are noted with the exception of the one data point indicated. The uncertainties in the quantities derived from the probe measurements can be judged from the following: The two cylindrical probes (at the most upstream and downstream traverse positions) were traversed across two blade spaces. The two probes were then interchanged and the traverses were repeated. The maximum variation in the properties derived from each blade space and each probe position (4 cases) was found to be 7.3 percent in the loss coefficient, 3.3 percent in the diffusion factor, and 0.67 percent in the AVDR.

Static Pressure Recovery. The static pressure was obtained

Downloaded From: http://turbomachinery.asmedigitalcollection.asme.org/ on 09/03/2013 Terms of Use: http://asme.org/terms

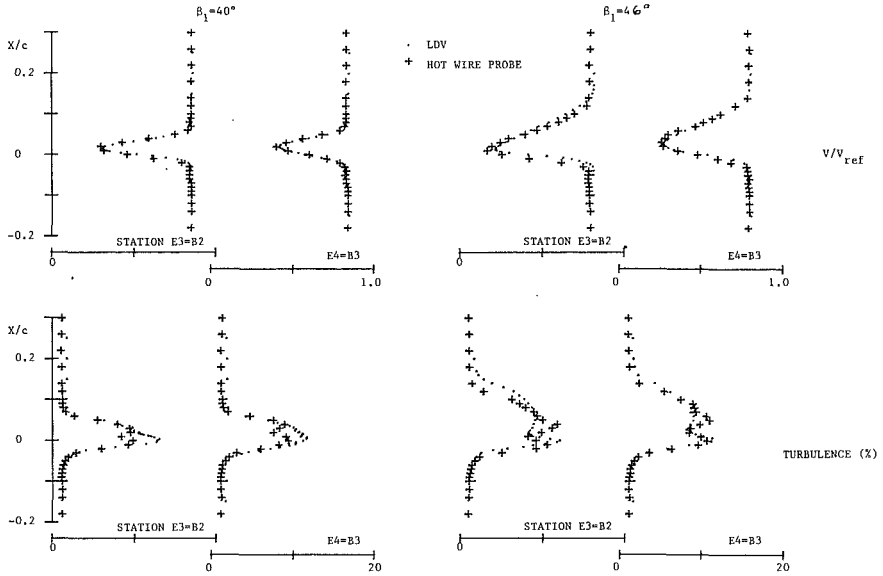

Fig. 6 Comparison of hot-wire and LDV wake measurements

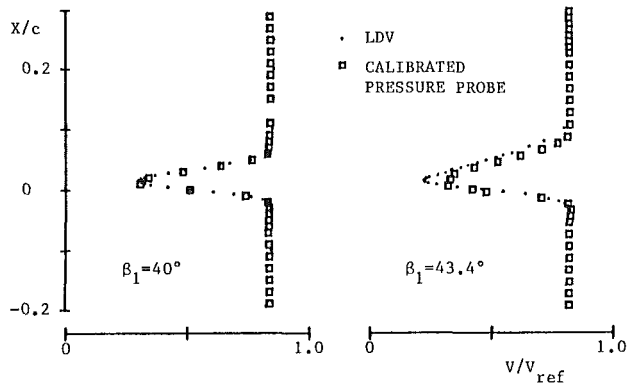

Fig. 7 Comparison of wake velocity profiles from LDV and calibrated pressure probe measurements at station E3 = D1

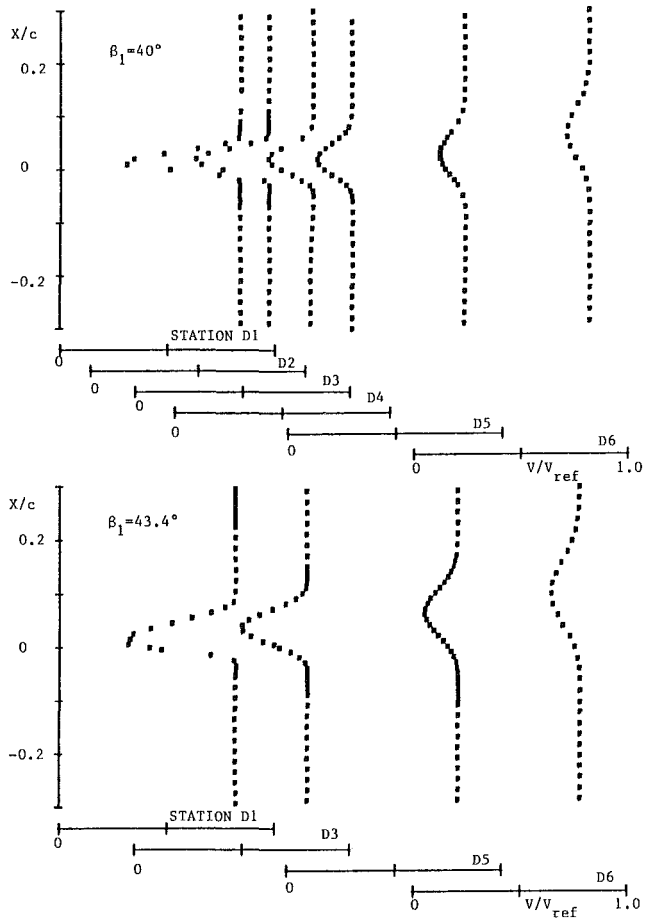

Fig. 8 Wake velocity distributions from calibrated pressure probe measurements

from the calibrated pressure probe at each point in the survey. Compared with the velocity and stagnation pressure variation through the wake, the variation in the static pressure was small. An example of the indicated static pressure variation through the wake is shown for $\beta_1 = 43.4$ deg in Fig. 11.

The static pressure variation was associated with a flow angle variation, which is shown in Fig. 12. [The flow angle was derived from the nonintrusive LDV measurements. However, the qualitative behavior of the flow angle through the wake seen in Fig. 12 was confirmed by Dreon (1986) using a special flow angle probe designed for shear layers.] It is also noted that the static pressure level outside the wake increased progressively, moving downstream of the trailing edge.

The degree to which the pressure level changed downstream of the blading is illustrated in Fig. 13. On this figure are shown the pressures measured on the surfaces of the blading in relation to the static pressure measured by the probe at the upper traverse station nearly 1.8 chord lengths downstream (station D6 in Fig. 2). It is evident that the static pressure rise downstream of the trailing edge was a very significant fraction (~ 30 percent) of the overall pressure rise across the cascade. The accuracy of this somewhat surprising observation was immediately questioned. However, calculations of losses from the very detailed LDV measurements alone had not proved successful because it was found that the assumption of static pressure level determined the loss magnitude.

The relationship of the static pressure rise and loss coefficient can be appreciated most easily by assuming the flow to be

Fig. 9 Location of the wake minimum velocity from LDV and calibrated pressure probe measurements

Downloaded From: http://turbomachinery.asmedigitalcollection.asme.org/ on 09/03/2013 Terms of Use: http://asme.org/terms

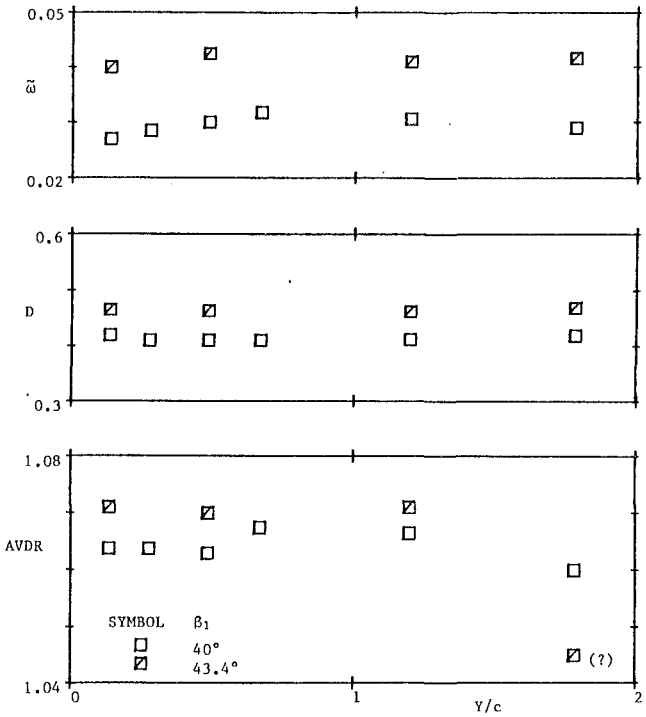

Fig. 10 Loss coefficient, diffusion factor, and AVDR from probe surveys at six downstream stations

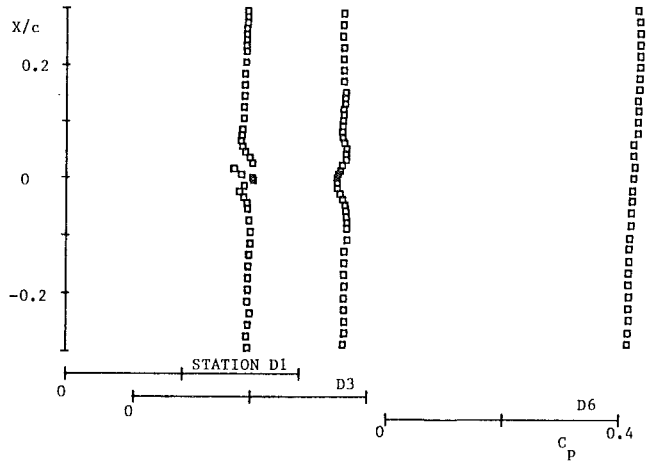

Fig. 11 Static pressure rise coefficient measured by the calibrated pressure probe in the wake at $\beta_1 = 43.4$ deg

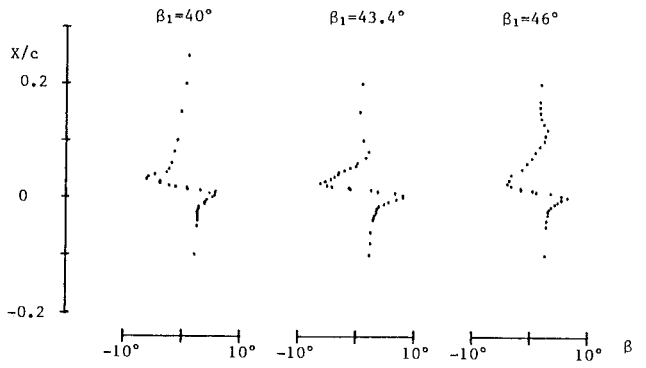

Fig. 12 LDV measurements of the flow angle in the wake at station E3

incompressible and fully mixed out at station D6. Then, the pressure rise coefficient is given by:

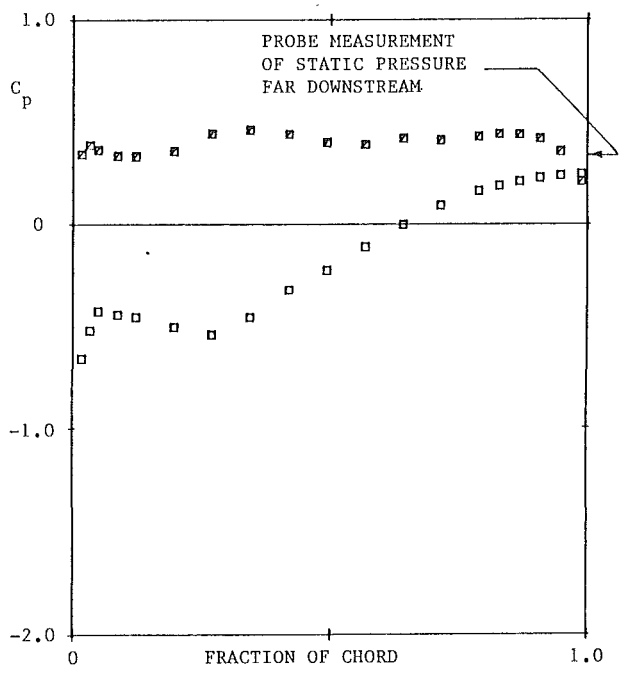

Fig. 13(*a*) Blade surface pressure at midspan for $\beta_1 = 40$ deg

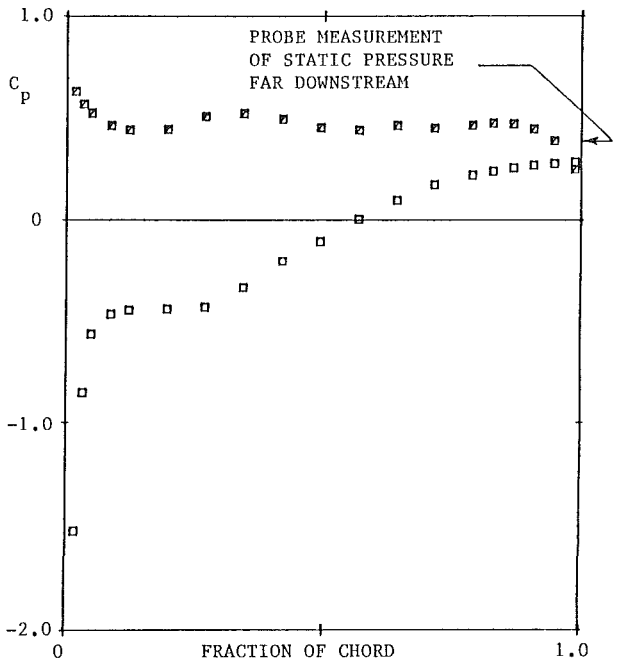

Fig. 13(*b*) Blade surface pressure at midspan for $\beta_1 = 43.3$ deg

$$C_{p2} = \frac{P_2 - P_1}{q_1} = \frac{P_{t2} - P_{t1}}{q_1} - \frac{\frac{1}{2}\rho(V_2^2 - V_1^2)}{q_1} = 1 - \frac{V_2^2}{V_1^2} - \tilde{\omega} \quad (1)$$

or

$$C_{p2} = 1 - (\text{AVDR})^2 \left(\frac{\cos\beta_1^2}{\cos\beta_2^2}\right) - \tilde{\omega} \quad (2)$$

The mixing-out process from the trailing edge is illustrated in Fig. 14. One blade space is shown with boundary layer displacement thicknesses of δ_s^* and δ_p^* on the suction and pressure sides, respectively. Conservation of momentum and mass for constant area axial flow gives

$$\frac{P_2 - P_{te}}{\frac{1}{2}\rho V_2^2} = 2\left[\frac{s}{s - (d_{te} + \delta_s^* + \delta_p^*)} - 1\right] \quad (3)$$

so that

Downloaded From: http://turbomachinery.asmedigitalcollection.asme.org/ on 09/03/2013 Terms of Use: http://asme.org/terms

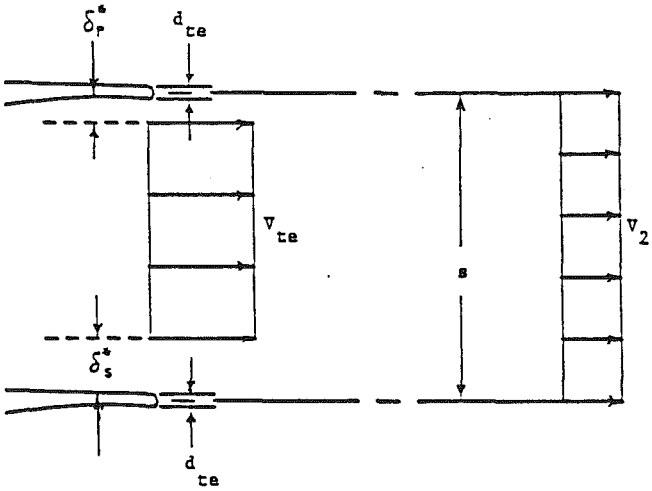

Fig.14 Illustration of the mixing analysis

$$C_{p2} = C_{pte} + \left[\frac{P_2 - P_{te}}{\frac{1}{2}\rho V^2_1}\right]\left[\frac{V_1^2}{V_2^2}\right] = C_{pte} + \Delta \tag{4}$$

where

$$\Delta = 2\left[\frac{k\sigma}{1-k\sigma}\right](\mathrm{AVDR})^2\left(\frac{\cos\beta_1}{\cos\beta_2}\right)^2 \tag{5}$$

and

$$k = \frac{d_{te}}{c} + \frac{\delta_s^*}{c} + \frac{\delta_p^*}{c} \tag{6}$$

The following table gives the results of calculating c_{p2} using equation (4), using LDV measurements of δ_s^* and δ_p^* and probe measurements of AVDR and β_2. The result is compared with the probe measurements of C_{p2} far downstream and C_{p2} evaluated using equation 2:

β_1(deg)		40	43.4
β_2(deg)	From cylindrical	2	2
AVDR	probe, far	1.065	1.07
$\tilde{\omega}$	downstream	0.029	0.042
δ_s^*/c	From LDV	0.0189	0.0286
$\delta_p{}^*/c$	surveys	0.0035	0.0027
d_{te}/c		0.025	0.025
k	From equation (6)	0.0474	0.0563
Δ	From equation (5)	0.1146	0.1256
C_{pte}	Average of pressure and suction surface taps	0.224	0.263
C_{p2}	From equation (4)	0.339	0.389
C_{p2}	From probe	0.32–0.34	0.37–0.39
C_{p2}	From equation (2)	0.310	0.354

Clearly the static pressure rise downstream of the trailing edge is consistent with the mixing of the boundary layers in the wake of the blade.

The difficulty in evaluating the loss purely from LDV measurements of velocity can be seen by rewriting equation (1) as

$$\tilde{\omega} = 1 - \frac{V_2^2}{V_1^2} - C_{p2} = \left[1 - \frac{V_2^2}{V_1^2}\right] - [C_{pte} + \Delta] \tag{7}$$

The LDV evaluates the first bracketed term (by integration in the nonuniform case) very accurately. However, the loss coefficient is a relatively small difference between the two much larger (bracketed) terms on the right-hand side. At any specific wake station, the value of Δ in the second term can be up to 30 percent of the term itself. Thus a reasonable assumption as to the magnitude of Δ (as a percentage of its value) can easily lead to an error in $\tilde{\omega}$ that is comparable in magnitude to its value. In contrast, the loss coefficient evaluated from the pressure probe measurements is the difference between weighted averages of measured stagnation pressure distributions. While the probe calibration for velocity enters into the calculation because the weighting factor is the local mass flux, the result depends to first order upon the direct measurement of stagnation pressure.

Thus it is argued that while LDV measurements are used widely to obtain velocity data for code verification purposes, viscous codes can not be validated using LDV data alone.

Since an important function of the code is to predict the losses, accurate measurements of losses must also be made in the experiment. In the absence of such measurements, numerical losses generated by the code can easily be reconciled with the velocity data through a seemingly reasonable assumption as to the pressure field.

Conclusions

Measurements have been obtained of the flow and losses in a controlled diffusion compressor cascade that provide an unusual test case for viscous code calculations. Of significance to code validation are the following features found to be present as the inlet air angle was progressively increased:

1 a laminar leading-edge separation, turbulent reattachment bubble on the suction side of the blade, with reattachment moving progressively downstream;

2 natural transition on the pressure side of the blade;

3 no further separation ahead of the trailing edge to angles at which losses exceeded four times the minimum for the cascade;

4 a "simple" wake developing from fully attached boundary layers at the trailing edge. [It is noted that Baydar (1988) showed from a spectral analysis of the hot-wire signal that vortex-shedding was not present at $\beta_1 = 40$, 46, and 48 deg. Vortex shedding was shown to occur at specific flow velocities at flow angles corresponding to negative incidence in earlier tests (Sanger and Shreeve, 1986).]

In obtaining data to be used for the validation of viscous code predictions of losses, it is important to measure the pressure field and the velocity field with equal precision.

The following were concluded in relation to blade design:

1 The off-design performance of the Sanger cascade showed that trailing edge separation can be avoided by design and need not develop automatically as a result of increasing incidence. [The adverse gradient downstream of reattachment was found to decrease with increasing incidence while the suction under the separation intensified (Elazar and Shreeve, 1990).] While this is an attractive off-design characteristic, it might disappear if the separation bubble (which contributes to the losses) was eliminated or reduced by redesign.

2 If the flow can be designed to remain attached to the trailing edge, the trailing edge geometry, in principle, can be shaped to maximize pressure recovery and minimize losses due to mixing. Better understanding of the near-wake region of a highly loaded cascade and further development of viscous computational ability are required for such an optimization. However, it is clear even now that the thickness of the blade at the very trailing edge contributed a predictable increment to the losses.

Downloaded From: http://turbomachinery.asmedigitalcollection.asme.org/ on 09/03/2013 Terms of Use: http://asme.org/terms

Acknowledgments

The present study was supported by the Naval Air Systems Command as part of the Air Breathing Propulsion Research Program under George Derderian. The program also benefitted from the early support and continuing interaction with Nelson Sanger at NASA Lewis Research Center.

References

Baydar, A., 1988, "Hot-Wire Measurements of Compressor Blade Wakes in a Cascade Wind Tunnel," M. S. Thesis, Naval Postgraduate School, Monterey, CA.

Classick, M., 1989, "Off-Design Loss Measurements in a Compressor Cascade," M. S. Thesis, Naval Postgraduate School, Monterey, CA.

Davis, R. L., Hobbs, D. E., and Weingold, H. D., 1988, "Prediction of Compressor Cascade Performance Using a Navier-Stokes Technique," ASME JOURNAL OF TURBOMACHINERY, Vol. 110, No. 4, pp. 520-531.

Deutsch, S., and Zierke, W. C., 1987, "The Measurement of Boundary Layers on a Compressor Blade in Cascade: Part 1—A Unique Experimental Facility," ASME JOURNAL OF TURBOMACHINERY, Vol. 109, pp. 520-526.

Deutsch, S., and Zierke, W. C., 1988 "The Measurement of Boundary Layers on a Compressor Blade in Cascade: Part 2—Suction Surface Boundary Layers," ASME JOURNAL OF TURBOMACHINERY, Vol. 110, pp. 138-145.

Deutsch, S., and Zierke, W. C., 1988, "The Measurement of Boundary Layers on Compressor Blade in Cascade: Part 3—Pressure Surface Boundary Layers and the Near Wake," ASME JOURNAL OF TURBOMACHINERY, Vol. 110, pp. 146-152.

Dreon, J. W., 1986, "Controlled Diffusion Compressor Blade Wake Measurements," M. S. Thesis, Naval Postgraduate School, Monterey, CA.

Elazar, Y., 1988, "A Mapping of the Viscous Flow Behavior in a Controlled Diffusion Compressor Cascade Using Laser Doppler Velocimetry and Preliminary Evaluation of Codes for the Prediction of Stall," Ph.D. Thesis, Naval Postgraduate School, Monterey, CA.

Elazar, Y., and Shreeve, R. P., 1990, "Viscous Flow in a Controlled Diffusion Compressor Cascade With Increasing Incidence," ASME JOURNAL OF TURBOMACHINERY, Vol. 112, pp. 256-266.

Hobbs, D. E., Wagner, J. H., Dannenhoffer, J. F., and Dring, R. P., 1982, "Experimental Investigation of Compressor Cascade Wakes," ASME Paper No. 82-GT-299.

Hobbs, D. E., and Weingold, H. D., 1984, "Development of Controlled Diffusion Airfoil for Multi-stage Compressor Applications," ASME *Journal of Engineering for Gas Turbines and Power*, Vol. 106, pp. 371-378.

McCormick, D. C., Patersen, R. W., and Weingold, H. D., 1988, "Experimental Investigation of Loading Effects on Simulated Compressor Airfoil Trailing Edge Flowfields," AIAA Paper No. 88-0365.

McNally, W. D., 1970, "Fortran Program for Calculating Compressible Laminar and Turbulent Boundary Layers in Arbitrary Pressure Gradients," NASA TN D-5681.

Murray, K. D., 1989, "Automation and Extension of LDV Measurements of Off-Design Flow in a Subsonic Cascade Wind Tunnel," A. E. Thesis, Naval Postgraduate School, Monterey, CA.

Patersen, R. W., and Weingold, H. D., 1985, "Experimental Investigation of a Simulated Compressor Trailing Edge Flow Field," *AIAA Journal*, Vol. 21, No. 5, pp. 768-775.

Sanger, N. L., 1983, "The Use of Optimization Techniques to Design Controlled-Diffusion Compressor Blading," ASME *Journal of Engineering for Power*, Vol. 105, pp. 256-264.

Sanger, N. L., and Shreeve, R. P., 1986, "Comparison of Calculated and Experimental Cascade Performance for Controlled Diffusion Compressor Stator Blading," ASME JOURNAL OF TURBOMACHINERY, Vol. 108, pp. 42-50.

Sanz, J. M., 1988, "Automated Design of Controlled Diffusion Blades," ASME JOURNAL OF TURBOMACHINERY, Vol. 110, pp. 540-544.

Shamroth, S. J., McDonald, H., and Briley, W. R., 1984, "Prediction of Cascade Flow Fields Using the Averaged Navier-Stokes Equations," ASME *Journal of Engineering for Gas Turbines and Power*, Vol. 106, pp. 383-390.

Shreeve, R. P., and Elazar, Y., 1989, "Laser Doppler Velocimeter Data From a Controlled Diffusion Compressor Cascade for Viscous Code Validation," Technical Report, NPS 67-89-001, Naval Postgraduate School, Monterey, CA (in preparation).

Snir, Z., 1988, "Investigation of Incompressible Cascade Flows Using a Viscous/Inviscid Interaction Code," M.S. Thesis Naval Postgraduate School, Monterey, CA.

Zierke, W. C., and Deutsch, S., 1990, "The Measurement of Boundary Layers on a Compressor Blade in Cascade: Part 4—Flow Fields for Incidence Angles of −1.5 and −8.5 Degrees," ASME JOURNAL OF TURBOMACHINERY, Vol. 112, pp. 241-255.

Downloaded From: http://turbomachinery.asmedigitalcollection.asme.org/ on 09/03/2013 Terms of Use: http://asme.org/terms